
Increased stratospheric resolution in the ECMWF forecasting system

Reprinted from ECMWF Newsletter Number 82

The Centre has been developing versions of its model and data assimilation system with finer and more extensive vertical resolution in both the stratosphere and the planetary boundary layer. In particular, 50- and 60-level versions (differing primarily in their boundary-layer resolution) are being extensively tested in data-assimilation, forecasting and multi-year simulations. The 50-level version is currently undergoing near-real-time trials with a view to early operational implementation, and replacement by the 60-level version is expected later in the year. Indications of some of the substantial improvements found in stratospheric analyses and forecasts are given here. We briefly describe a simple new parametrization of upper-stratospheric moistening by methane oxidation, and discuss the overall simulation of stratospheric humidity, which is strongly dependent on the accuracy of the thermal and dynamical representation of the stratosphere.

The revised versions of the forecasting system

The ECMWF model uses a hybrid vertical coordinate that reduces smoothly from a terrain-following coordinate in the lower troposphere to a pressure coordinate in the stratosphere (Simmons and Burridge, 1981; Simmons and Strüfing, 1983). Since September 1991, a 31-level resolution has been used operationally (Ritchie et al., 1995), with levels distributed as shown in the left-hand portion of Fig. 1. The top four levels are located at pressures of exactly 10, 30, 50 and 70 hPa, and the pressures at the next two levels are very close to 90 and 110 hPa.

The 50-level version of the model is illustrated in the right-hand portion of Fig. 1. The distribution of levels is the same as in the 31-level version below 150 hPa, and levels between 60 and 5 hPa are close to equally-distributed in height with a spacing of 1.5 km. The spacing increases above the 5 hPa level and the top level is at 0.1 hPa.

While this 50-level version of the model was being developed, an independent study of increased vertical resolution in the planetary boundary layer and lower troposphere was yielding promising results (Teixeira, 1999). This led to construction of the 60-level version of the model, with stratospheric resolution similar to that of the 50-level version (but with minor rearrangement of levels), and with much finer resolution in the planetary boundary layer and immediately above. This will form the basis for further developments, as summarized in the concluding section of this article.

A number of problems had to be addressed in developing the versions of the forecasting system with improved stratospheric resolution, and these versions have benefited also from some other recent developments of the forecasting system. Several of the beneficial changes have already been introduced operationally. These include revisions of the radiative parametrization, the two-time-level semi-Lagrangian advection scheme, the calculation of saturation specific humidity at low temperatures, the analysis of humidity and the specification of the ozone climatology.

Several other changes have been included in the experimental 50- and 60-level systems. Rayleigh friction has been introduced at the uppermost few model levels to ensure a broadly realistic simulation of the mean circulation close to the stratopause. Changes have been made to parameters in the semi-implicit scheme to remove noise arising from weak computational instabilities. Nonlinear normal-mode initialization has been suppressed in the incremental 4D-Var data assimilation (Rabier et al., 1999) to avoid large initialization changes at high levels arising from large normal-mode amplitudes at low pressures. In addition, the model has been enhanced by introduction of the parametrization of methane oxidation specified later in this article.

It was also necessary to compute new sets of balance operators and background error covariances for the data assimilation (Bouttier et al., 1997). These are derived in general from sets of differences between two- and one-day forecasts verifying at the same time. The first set of 50-level forecasts used for these calculations was made from initial conditions formed by merging 31-level ECMWF analyses with UKMO stratospheric analyses (Swinbank and O'Neill, 1994). Implied upper-level errors were reduced to counter effects of incompatibilities between the ECMWF model and the UKMO analyses. These background statistics were used for two periods of data assimilation and forecasts. A revised set of statistics was then computed from these 50-level forecasts.

General performance of 50-level system

Data assimilation has been carried out continuously since 15 May 1998 with one form or other of the 50-level system, and 50-level assimilations have also been run for December 1997 and most of January 1998. Objective verification shows that the enhanced resolution provides substantially better stratospheric analyses and forecasts at the levels up to 10 hPa where comparison can be made with results from the standard 31-level system. Fits of 30 hPa temperatures and winds to northern-hemisphere radiosonde measurements are presented in Fig. 2. They are averaged over 165 days of experimentation run with the original background statistics; 50-level experiments for shorter periods using the revised background statistics give slightly better results still. The 50-level analyses (day 0) and forecasts (throughout the range to day 10) can be clearly seen in Fig. 2 to be

closer to the verifying radiosonde data than the 31-level analyses and forecasts. Similar plots for other areas and stratospheric levels, and for verification against analyses, confirm the superior performance of the 50-level system. The only notable exception is in the tropical stratosphere, where the 50-level forecasts exhibit a larger growth of bias in temperature, although temperature analyses (and wind analyses and forecasts) are nevertheless better from the 50-level system.

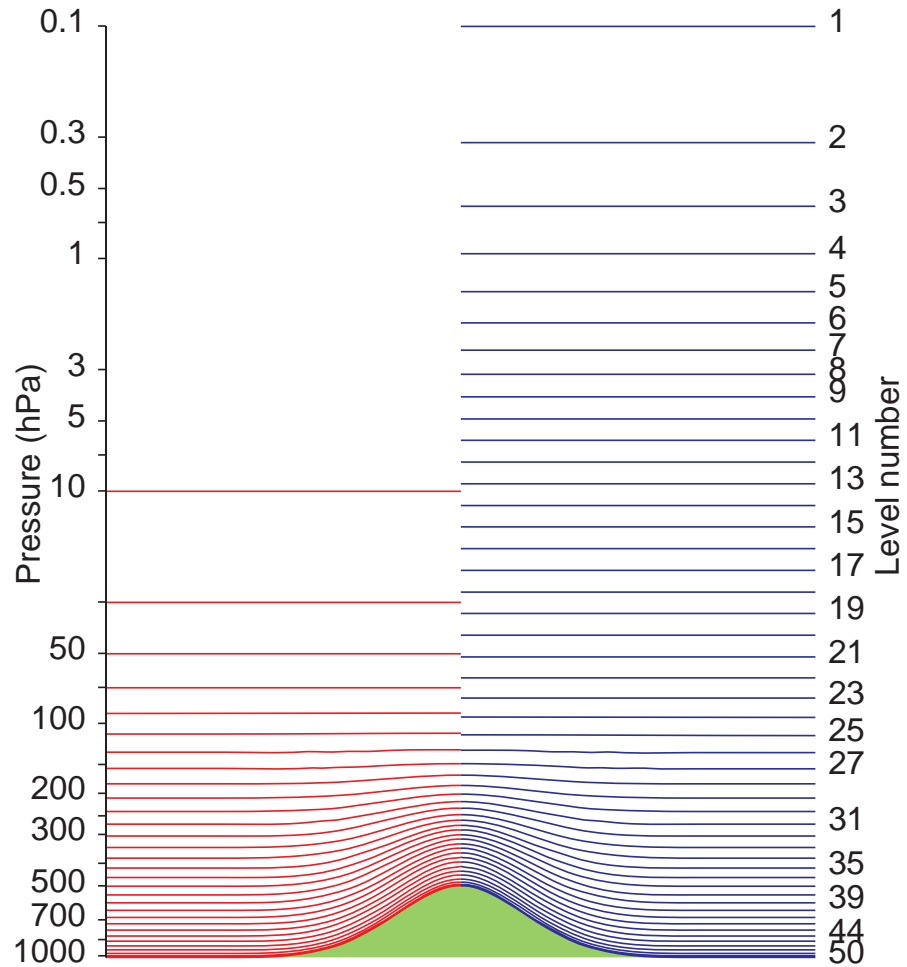


Fig. 1 The distribution of the full model levels at which wind, temperature and humidity are represented, for 31-level (left) and 50 level (right) vertical resolutions, plotted for surface pressures which vary from 1013.25 to 500 hPa.

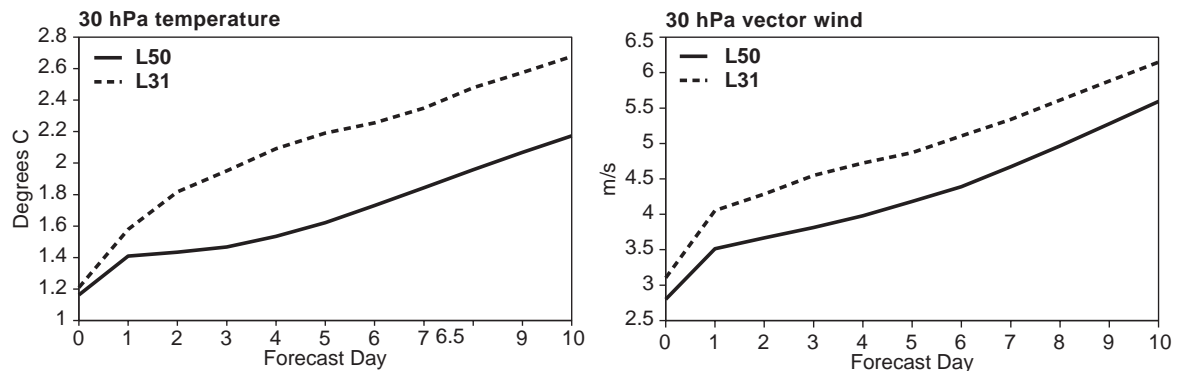


Fig. 2 Root-mean-square errors of 30 hPa temperature and vector-wind analyses (day 0) and forecasts (days 1 to 10) verified against radiosonde measurements over the extratropical northern hemisphere, averaged over a set of 165 cases run with 50-level (red, solid) and 31 level (blue, dotted) vertical resolutions.

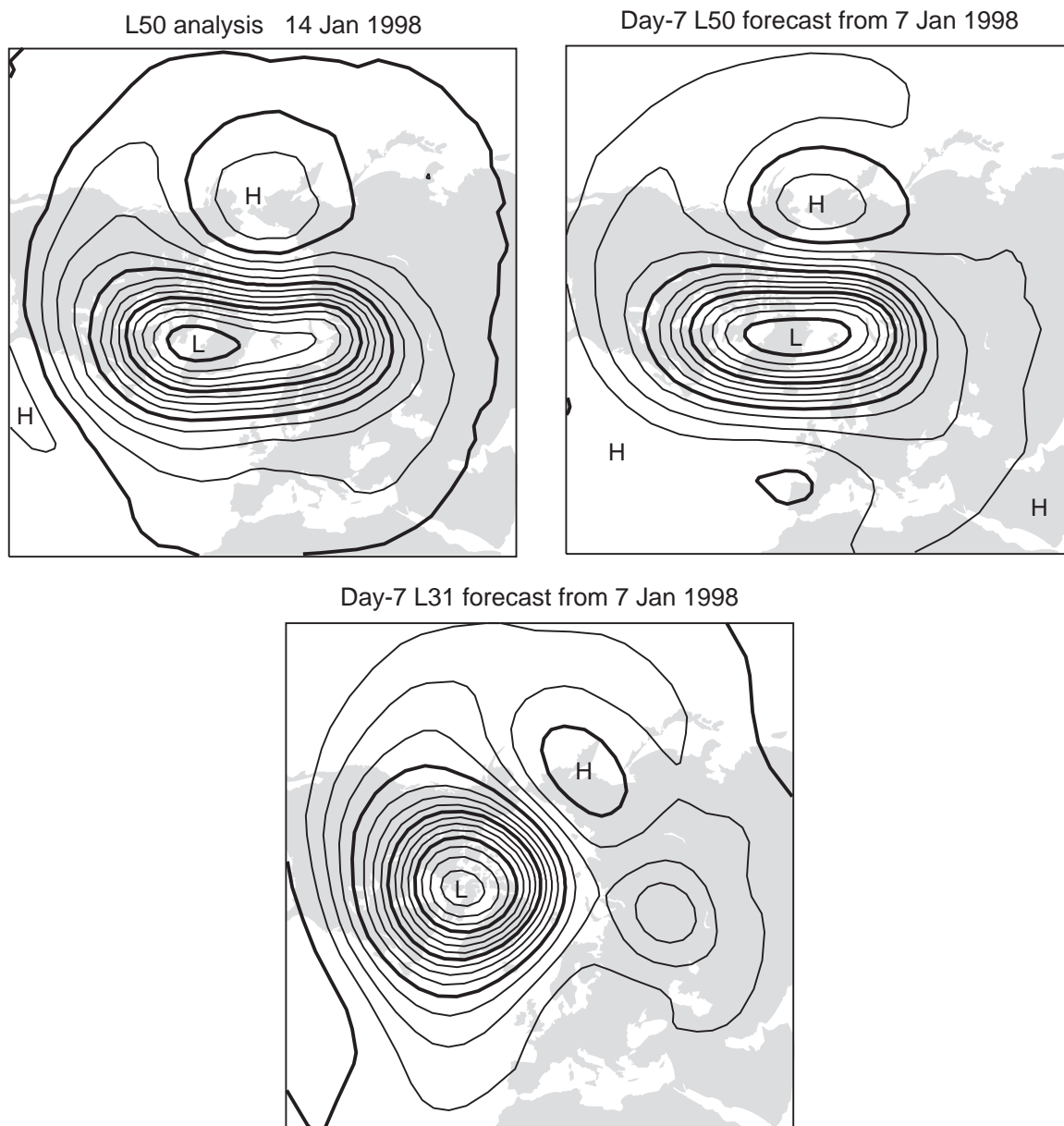


Fig. 3 The 10 hPa height analysis for 12UTC 14 January 1998 from the 50-level version (upper left), and seven-day forecasts verifying on this date from the 50-level (upper right) and 31-level (lower) versions of the forecasting system. The contour interval is 160 m.

Synoptic study of wintertime stratospheric forecasts also clearly demonstrates that the 50-level system performs better than the 31-level system. The upper panel of Fig. 3 shows the analysis at 10 hPa from the 50-level system for a day on which there was a marked elongation of the polar vortex. The corresponding analysis from the 31-level system (not shown) is very similar. The seven-day forecast verifying on this day from the 50-level system (middle panel) captured quite accurately the elongation of the vortex, whereas the 31-level system (lower panel) erroneously predicted a strong vortex centred over northern Canada and a weaker circulation over Siberia. This is a pronounced case, but the stratospheric forecasts from the 50-level version (or indeed from the 60-level version) are found almost invariably to be better synoptically than those from the 31-level version in depicting features such as the strength and position of the Aleutian high or the shape and orientation of the polar vortex. Dramatic synoptic improvements during a period of major early-winter polar warming have been seen recently in the near-real-time trial of the 50-level system.

Fig. 4 shows the zonal-mean zonal flow for October 1998 from the 50-level analyses and from the UKMO stratospheric analyses. Tropospheric differences should be disregarded, as the averaging was performed on model coordinate surfaces (terrain-following in the troposphere) for the ECMWF analyses and on pressure surfaces for the UKMO analyses. There is a reassuring agreement between the two mean stratospheric analyses in the extratropics, where the only difference of

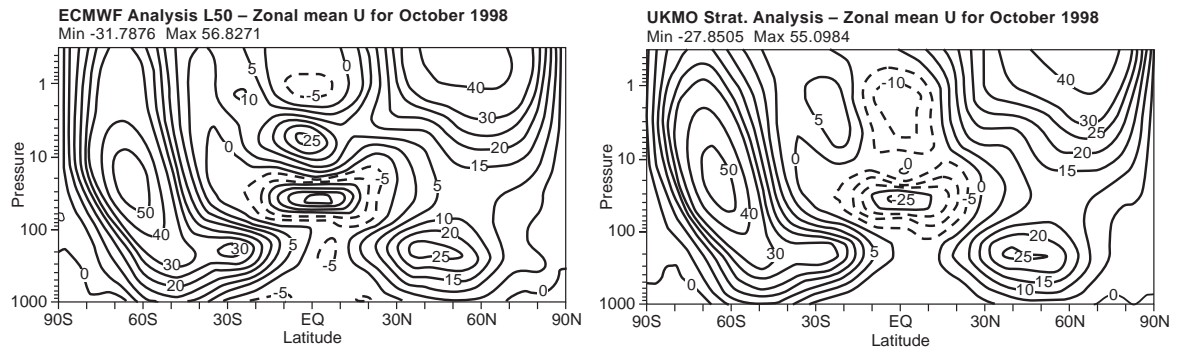


Fig. 4 Meridional cross-sections of zonal-mean zonal wind averaged for the month of October 1998 from experimental 50-level ECMWF analyses (left) and from the stratospheric analysis system of UKMO (right). Red contours denote westerlies, blue contours easterlies, and the contour interval is 5 ms⁻¹. Tropospheric differences should be disregarded.

note occurs close to the stratopause in the southern hemisphere. Differences are, however, more marked in the tropics. The easterly maximum located at about 40 hPa is more than 5 ms⁻¹ stronger in the ECMWF analysis, and this analysis has westerlies of up to 25 ms⁻¹ above 10 hPa, where the UKMO analysis has easterlies. It is not surprising that differences are large in this region, because of difficulty in modelling the quasi-biennial oscillation (QBO) because of the paucity of wind observations, and because of the limited extent to which the wind analyses in the tropics can be controlled by assimilation of satellite radiance measurements. There is evidently a need for further study of the realism of the tropical stratospheric wind analyses from the new system, particularly to examine performance over a complete cycle of the QBO.

Figure 5 presents objective verification of 500 hPa height forecasts from the 50- and 31-level systems. It is based on the extensive sets of forecasts available with the original background statistics; the average is over the 154 forecasts that can be verified against analyses produced using the same model version that provided the initial conditions. The 50-level version gives better mean verification scores throughout the medium range. Although differences appear small, they are in fact quite significant when interpreted in the context of the long-term evolution of forecast skill, which has seen an increase by the order of one day per ten years in the forecast range at which the anomaly correlation falls below 60%.

Repeating a subset of the forecasts included in Figure 5 using the revised background statistics yields very similar hemispheric verification scores for the 50-level system, but some marked regional differences. In particular, much less improvement was found over Europe with the revised background statistics, whereas the converse was the case for North America. Further study of the specification of the background statistics is evidently needed and is planned (see later). For the time being, the 50-level system with revised background statistics currently undergoing near-real-time parallel trials is expected to yield substantial improvements in operational stratospheric products and some small improvement in tropospheric products, with further improvements expected from additional work to be carried out after operational implementation.

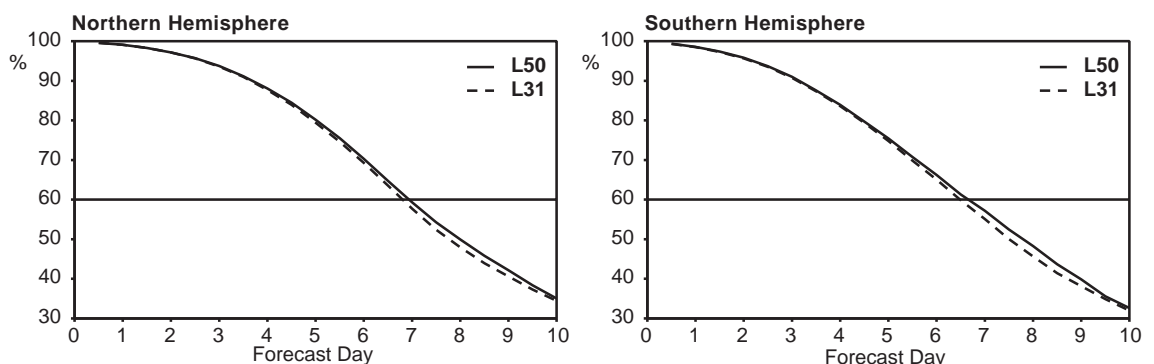


Fig. 5 Anomaly correlations of 500 hPa height averaged over 154 cases run with 50-level (solid) and 31-level (dashed) vertical resolutions, for the extratropical northern (left) and southern (right) hemispheres.

The treatment of methane oxidation

ECMWF analyses and simulations have typically been too dry in the stratosphere, because of the absence of a representation of the high-level source of water vapour due to the oxidation of methane (Simmons et al., 1999). This has been seen, for example, in a recent 19-year simulation using observed surface boundary conditions for the years 1979-1997, carried out as a contribution to the second phase of the Atmospheric Model Intercomparison Project (AMIP; Gates, 1992). A run of the 50-level version of the model using T63 horizontal resolution dried gradually over the first decade of integration, leading to upper stratospheric specific humidities around 1.7-1.8 mg/kg. These values were maintained over the second half of the integration period. This is not unreasonable in the absence of methane oxidation, as it corresponds to a long-term water-vapour mixing ratio of around 2.8 ppmv, giving a value of 6.2 ppmv when twice the tropospheric methane mixing ratio of 1.7 ppmv is added. Photochemical calculations and observations (e.g. Brasseur and Solomon, 1984; Bithell et al., 1994) indicate that the sum of the mixing ratio of water vapour and twice that of methane is approximately constant over much of the stratosphere, with a value close to or a little above 6 ppmv.

A simple parametrization of the moistening by methane oxidation has thus been developed. The basic assumptions are that the volume mixing ratio of water vapour $[H_2O]$ increases at rate $2k_1[CH_4]$ and that there is a steady balance between the mixing ratios of methane and water vapour:

$$2[CH_4] + [H_2O] = 6 \text{ ppmv}$$

The rate of increase of water vapour (in ppmv) is then

$$k_1(6 - [H_2O])$$

In terms of specific humidity, q , the source is

$$k_1(Q - q)$$

where Q has the value 3.75 mg/kg.

For completeness, an extra photolysis term $-k_2q$ is included in the mesosphere, although it has little effect for the 50- and 60-level resolutions discussed here.

k_1 and k_2 are specified as functions of pressure, with k_1 equal to $(100 \text{ days})^{-1}$ at pressures less than 1 hPa. The vertical profiles of k_1 and k_2 are chosen such that the dependence on altitude of the combined photochemical lifetime, $(k_1 + k_2)^{-1}$, shown in Figure 6, is similar to that presented by Brasseur and Solomon (1984). The slow time scale of the process in the stratosphere enables latitudinal and temporal variations in relaxation rate to be neglected in the first instance.

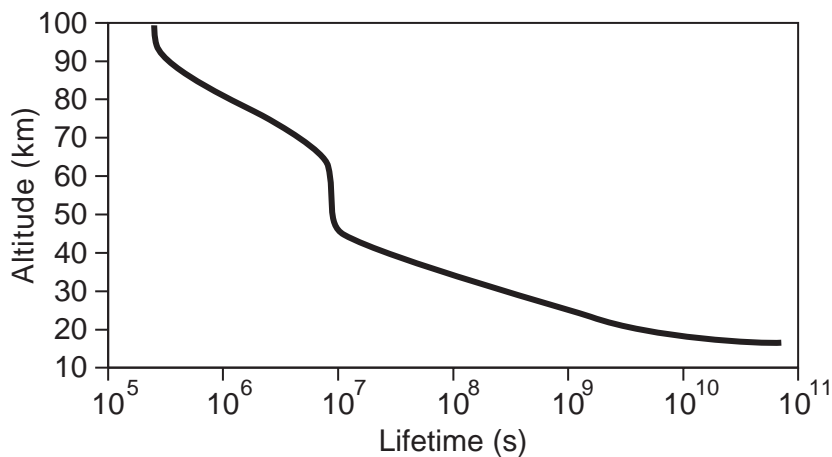


Fig. 6 Combined photochemical lifetime

Stratospheric humidity in simulations and analyses

A new AMIP simulation including the parametrization of methane oxidation has been run using the 60-level vertical resolution. After an initial adjustment period of several years, the stratospheric humidity in this simulation exhibits a fairly regular annual cycle. Latitude/pressure sections showing 15-year means for January, April, July and October are presented in Figure 7. These sections may be compared with observational data from the UARS satellite processed by Randel et al. (1998). The model successfully captures the dryness both of air entering the stratosphere in the tropics in the boreal winter and of air in the cold Antarctic lower stratosphere in austral winter and spring, this being consistent with realistic simulated temperatures at the tropical tropopause and in the polar winter stratosphere. The consequences of a general ascent of relatively dry air throughout the tropical stratosphere, and the net high-latitude wintertime descent

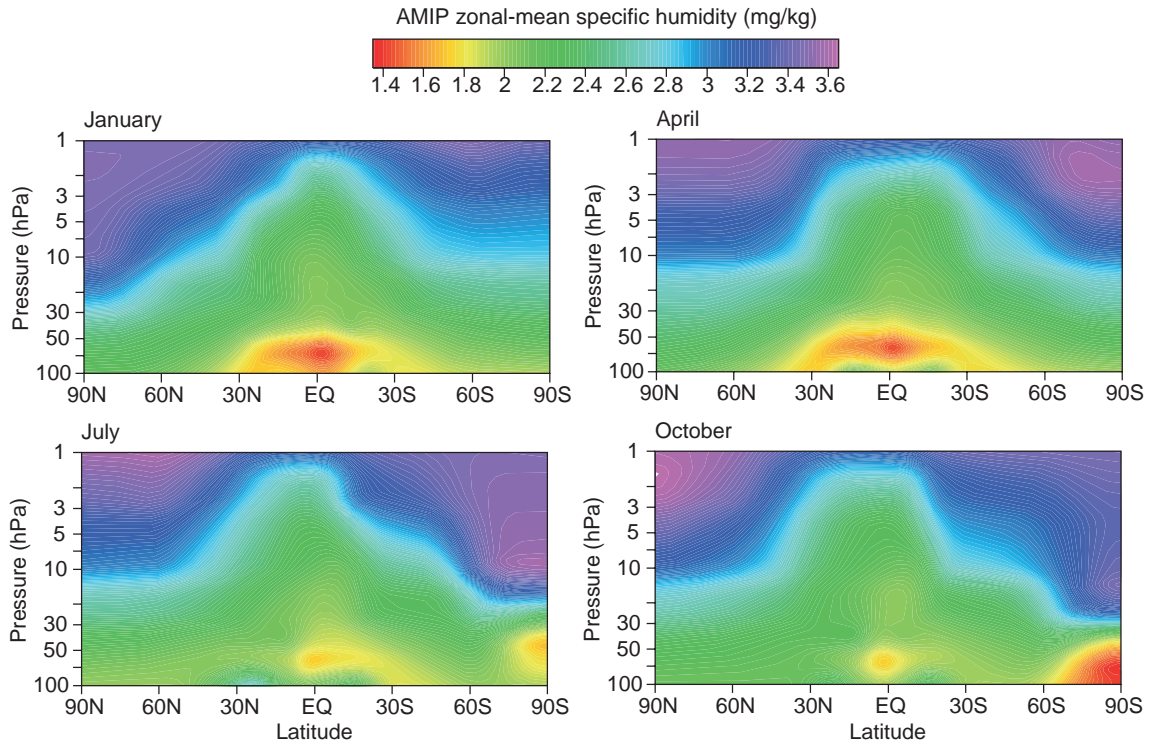


Fig. 7 Meridional cross-sections of zonal-mean specific humidity for January, April, July and October from a 60-level AMIP simulation. Each section is a 15-year average for 1983-1997.

(and summertime ascent) of air moistened by methane oxidation can be clearly seen. The model is unable to capture the observed dryness of the winter polar upper stratosphere as it does not have the resolution to describe correctly the wintertime descent of dry air from the mesosphere. It represents the upward tropical transfer of the annual cycle in water vapour (the “tape-recorder” effect discussed by Mote et al., 1996), but is generally too diffusive, and drier in the tropical middle stratosphere by some 10-20% compared with UARS data.

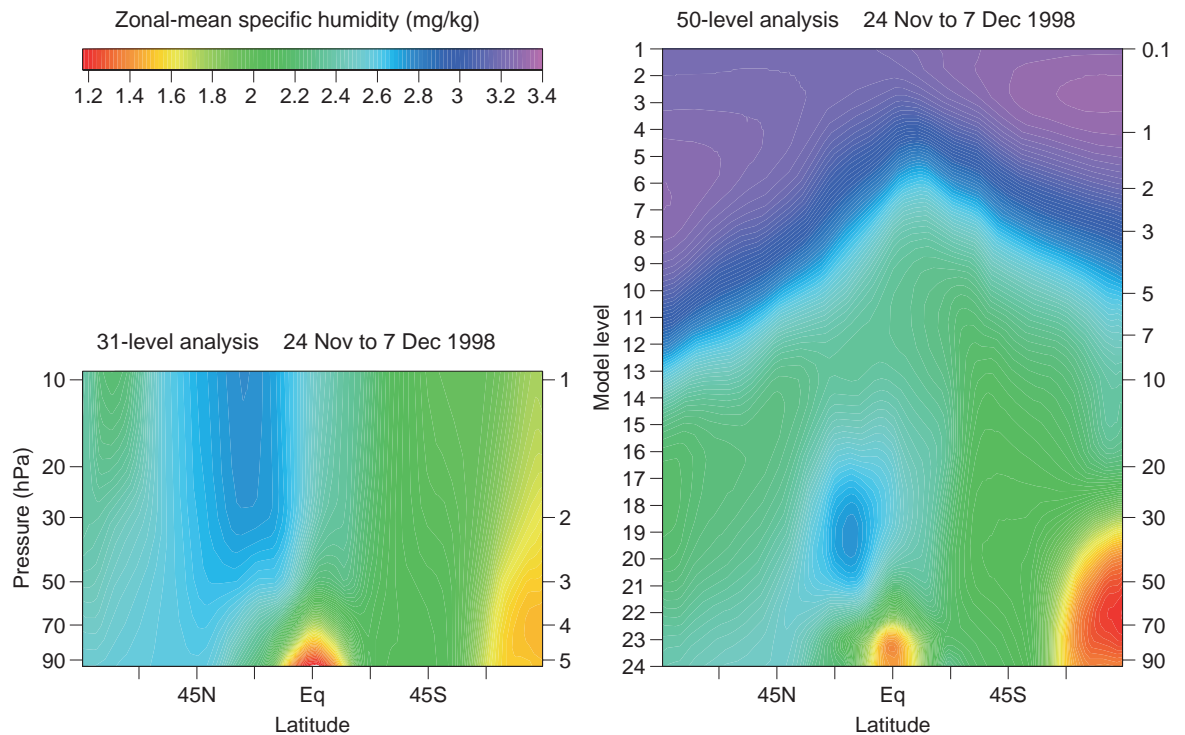


Fig. 8 Meridional cross-sections of zonal- and time-mean specific humidity from 31- and 50-level analyses.

No observations of stratospheric humidity are used in the ECMWF analysis system. Humidity simply evolves during the assimilation according to the model's dynamical and parametrized physical processes, with winds and temperatures (and tropospheric humidity) constrained by the analysis process. The parametrization of methane oxidation was activated on 17 June 1998 in the data assimilation cycles using the 50-level version of the model. The stratospheric analyses have not yet become fully adapted to the change, but it is nevertheless instructive to compare 31-level and 50-level analyses. Meridional cross-sections of zonal-mean specific humidity averaged over the last week of November and the first week of December are shown in Figure 8.

The parametrization of methane oxidation has had little effect below 10 hPa by the time shown in Figure 8. Lower stratospheric differences instead arise mostly from the resolution difference. The 31-level analyses generally exhibit a too rapid upward transfer of relatively moist or dry air introduced at the tropical tropopause (Simmons et al., 1999). 50-level simulations are found to be much more realistic in this respect, although upward transfer and attenuation in the deep tropics are still stronger than observed, as in the 60-level AMIP simulation discussed above. Figure 8 shows that the benefit seen in the high-resolution simulations carries over into the 50-level analyses. Relatively moist air was introduced into the stratospheric analyses in the boreal subtropics over the summer of 1998, and by December the maximum in humidity has reached 10 hPa in the 31-level analyses, but is still below 30 hPa in the 50-level analyses. The maximum is located further north in the 31-level system, and much more moistening of the northern extratropics has taken place in this system. At high southern latitudes, the 31-level system is moister than the 50-level system in the lower stratosphere, but drier at 10 hPa. The latter is due partly to colder 10 hPa temperatures (and more condensation) in winter and early spring in the 31-level system and partly to descent of moister air from the upper stratosphere in the 50-level system. By December, however, there is mean ascent at high southern latitudes, this acting to dry the middle stratosphere in this region and season.

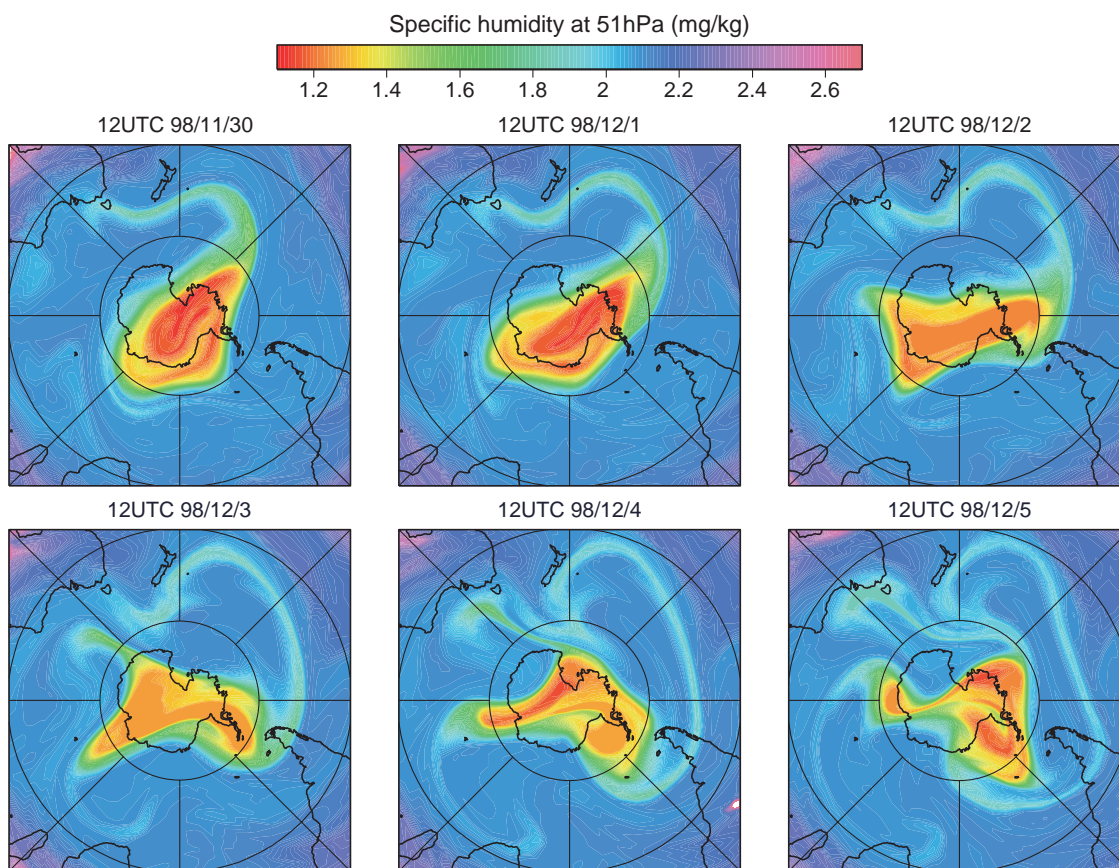


Fig. 9 Specific humidity at close to 51 hPa from 50-level analyses for consecutive days from 30 November to 5 December 1998

Daily analyses of humidity over the southern hemisphere from 30 November to 5 December 1998 are presented in Figure 9, for the model level close to 51 hPa from the 50-level system. The driest air is located in the decaying, perturbed westerly vortex, where dehydration by the parametrized condensation process occurred earlier when temperatures were sufficiently cold. The maps show evolving filamentary structure in the humidity field, and indications of mixing. Observations of fields which behave largely as passive tracers can be used effectively to extract information on the wind field in a 4D-Var assimilation system. This is a prime motivation for ongoing work to include stratospheric ozone as a variable of the ECMWF system.

Plans

Our immediate goal is the operational implementation of the 50-level version of the forecasting system. Included with this will be a new fast radiative transfer model for the assimilation of radiance data from satellites (Saunders et al., 1999). The availability of model background fields that cover the whole of the stratosphere as well as the troposphere will be exploited in a new scheme for the assimilation of raw radiances from the TOVS and new ATOVS instruments. It is expected that this scheme will be introduced into operations soon after the 50-level system.

Further development is being concentrated on the 60-level system. The specification of background error statistics will be investigated in conjunction with a revision of observation errors which addresses known deficiencies. Assimilation of ozone data will be added to the 60-level system. Operational implementation is planned for later this year. Work is also in hand to use the 60-level system for the new ECMWF reanalysis, ERA-40, covering the period from 1957 to the present day.

Acknowledgements

This work has been greatly facilitated by the use of stratospheric analyses made available by the UK Meteorological Office. Ideas and advice from Bob Harwood and colleagues at Edinburgh University on the representation of methane oxidation are gratefully acknowledged.

References

- Bithell, M., Gray, L.J., Harries, J.E., Russell, J.M.III, and Tuck, A.F.** (1994) Synoptic interpretation of measurements from HALOE. *J. Atmos. Sci.*, **51**, 2942-2956.
- Bouttier, F., Derber, J., and Fisher, M.** (1997) The 1997 revision of the Jb term in 3D/4D-Var. ECMWF Tech. Memo., 238, 54 pp.
- Brasseur, G., and Solomon, S.** (1984) *Aeronomy of the Middle Atmosphere*. D. Reidel Publishing Co., Dordrecht, 452 pp.
- Gates, W.L.** (1992) AMIP: The Atmospheric Model Intercomparison Project. *Bull. Amer. Meteorol. Soc.*, **73**, 1962-1970.
- Mote, P.W., Rosenlof, K.H., McIntyre, M.E., Carr, E.S., Gille, J.C., Holton, J.R., Kinnersley, J.S., Pumphrey, H.C., Russell, J.M. III, and Waters, J.W.** (1996) An atmospheric tape recorder: The imprint of tropical tropopause temperatures on stratospheric water vapour. *J. Geophys. Res.*, **101D**, 3989-4006.
- Rabier, F., Järvinen, H., Klinker, E., Mahfouf, and Simmons, A.** (1999) The ECMWF operational implementation of four dimensional variational assimilation. Part I: Experimental results with simplified physics. Submitted to *Q. J. R. Meteorol. Soc.*.
- Randel, W.J., Wu, F., Russell, J.M. III, Roche, A., and Waters, J.W.** (1998) Seasonal cycles and QBO variations in stratospheric CH₄ and H₂O observed in UARS HALOE data. *J. Atmos. Sci.*, **55**, 163-185.
- Ritchie, H., Temperton, C., Simmons, A., Hortal, M., Davies, T., Dent, D., and Hamrud, M.** (1995) Implementation of the semi-Lagrangian method in a high resolution version of the ECMWF forecast model. *Mon. Wea. Rev.*, **123**, 489-514.
- Saunders, R.W., Matricardi, M., and Brunel, P.** (1999) An improved fast radiative transfer model for assimilation of satellite radiance observations. *Q. J. R. Meteorol. Soc.*, **125**, in press.
- Simmons, A.J., and Burridge, D.M.** (1981) An energy and angular momentum conserving vertical finite-difference scheme and hybrid vertical coordinates. *Mon. Wea. Rev.*, **109**, 758-766.
- Simmons, A.J., and Strüfing, R.** (1983) Numerical forecasts of stratospheric warming events using a model with a hybrid vertical coordinate. *Q. J. R. Meteorol. Soc.*, **109**, 81-111.
- Simmons, A.J., Untch, A., Jakob, C., Källberg, P., and Undén, P.** (1999) Stratospheric water vapour and tropical tropopause temperatures in ECMWF analyses and multi-year simulations. *Q. J. R. Meteorol. Soc.*, **125**, in press.
- Swinbank, R., and O'Neill, A.** (1994) A stratosphere-troposphere data assimilation system. *Mon. Wea. Rev.*, **122**, 686-702.
- Teixeira, J.** (1999) The impact of increased boundary layer vertical resolution on the ECMWF forecast system. ECMWF Tech. Memo. 267.

Agathe Untch, Adrian Simmons and Colleagues

